Preprints of the 2012 20th Mediterranean Conference on Control & Automation (MED), Barcelona, Spain, July 3-6, 2012

Controller design for voltage regulation and stabilization in multimachine power systems

Giuseppe Fusco and Mario Russo, *Members IEEE*
Università degli Studi di Cassino e del Lazio Meridionale
via G. Di Biasio 43, 03043 Cassino (FR), Italy
{fusco,russo}@unicas.it

***Abstract*— This paper deals with the problem to guarantee system stability and voltage regulation in multimachine power systems. The power system is decomposed in n subsystems each one containing a synchronous generator. For each subsystem two input-output models of low order are derived modelling the electrical and mechanical dynamics, respectively. Each model presents parameter uncertainties and input disturbance. A voltage controller based on the internal model control is designed and sequentially a stabilizing controller (PSS) is designed so as to enhance swing damping. According to the decentralized approach, the controllers use only locally available measurements. Numerical simulation studies conducted on a three machine test power system show the performance obtained in the presence of severe contingencies.**

I. Introduction

In power systems control, the problem to improve transient stability and voltage regulation is a key issue to provide reliable and efficient operations of the transmission system. A short-circuit in power systems may not only cause the system losing synchronism but also result into short-term voltage dips. It is then important that the control system acts both to suppress the potential instability due to poorly damped power angle oscillations and to quickly restore the pre-fault voltage [1], [9].

The problem to guarantee transient stability is difficult to pursue in centralized control. In fact, due to the physical limitation on the system structure, a large amount of information exchanges between the control systems is usually unfeasible. These difficulties have motivated the use of different design techniques based on the decentralized control theory, see among them [2], [3], [4], [7], [8], [11], [14], [16].

From the modeling point of view, it is a common practice to regard a multimachine power system as a set of small interconnected subsystems, each one presenting a synchronous generator [5], [8], [13]. In this paper, each subsystem is represented by two input-output differential models representing the electrical and mechanical dynamics, respectively. Each model is developed without using linearization techniques. It is obtained by arranging the generator and the network models so as to representing nonlinearities by bounded time functions which concur to form uncertain parameters and unknown inputs disturbance of class L_∞.

A voltage controller and a stabilizing controller (PSS) are then sequentially designed. The voltage controller is designed according to the internal model control technique which ensures set-point regulation while giving robustness with respect to model uncertainties and disturbance rejection. Concerning the PSS, the stabilizing signal is an algebraic function of the electrical power and its first time derivative, so as to use only measurements of electrical quantities. The two gains of the PSS are designed with the aim to attenuate the effect of the disturbance thus improving the swing damping. Thanks to the low order of the mechanical model, some considerations are provided to guide the tuning of the two gains. It is important to remark that the advantage of a straight-forward design presents the drawback of a trade-off between the transient performance of voltage regulation and electro-mechanical damping. Numerical simulations show that the designed controllers exhibit acceptable performance both in terms of electromechanical oscillations damping and voltage regulation in presence of different locations of the three-phase short circuit.

II. Power System Model

Under standard assumptions, the dynamic model of a power system consisting of *n*-machines interconnected by a transmission network can be described as follows [1], [9]

$$\frac{\mathrm{d}\delta_i}{\mathrm{d}t}(t) = \Delta\omega_i(t) \tag{1}$$

$$\frac{\mathrm{d}\Delta\omega_i}{\mathrm{d}t}(t) = -\frac{D_i}{H_i}\,\Delta\omega_i(t) - \frac{\omega_0}{H_i}\,\Delta P_{ei}(t) \tag{2}$$

$$\frac{\mathrm{d}e'_{qi}}{\mathrm{d}t}(t) = -\frac{1}{T'_{d0i}}\Big(e'_{qi}(t) + (x_{di} - x'_{di})i_{di}(t) - k_{ci}\,v_{fi}(t)\Big) \tag{3}$$

where $i = 1 \dots n$ and

$$i_{di}(t) = \sum_{j=1}^{n} e'_{qj}(t)\,\alpha_{ij}(t) \tag{4}$$

$$i_{qi}(t) = \sum_{j=1}^{n} e'_{qj}(t)\,\beta_{ij}(t) \tag{5}$$

$$v_{di}(t) = x_{qi}\,i_{qi}(t) \tag{6}$$

$$v_{qi}(t) = e'_{qi}(t) - x'_{di}i_{di}(t) \tag{7}$$

$$v_i^2(t) = v_{qi}^2(t) + v_{di}^2(t) \tag{8}$$

978-1-4673-2529-5/12/$31.00 ©2012 IEEE

with

$$\alpha_{ij}(t) = -B_{ij}\cos\big(\delta_i(t) - \delta_j(t)\big)) \quad (9)$$

$$\beta_{ij}(t) = B_{ij}\sin\big(\delta_i(t) - \delta_j(t)\big). \quad (10)$$

The active electrical power is given by

$$P_{ei}(t) = v_{di}(t)\, i_{di}(t) + v_{qi}(t)\, i_{qi}(t)$$

which, using (6) and (7), can be rewritten as

$$P_{ei}(t) = \frac{v_{di}(t)\, e'_{qi}(t)}{x'_{di}} - \frac{x_{qi} - x'_{di}}{x_{qi}\, x'_{di}}\, v_{di}(t)\, v_{qi}(t). \quad (11)$$

In (1)-(10), $\delta_i(t)$ is the rotor angle; $\Delta\omega_i(t) = \omega_i(t) - \omega_0$ the speed deviation; $\omega_i(t)$ the rotor speed; ω_0 the synchronous speed; $\Delta P_{ei}(t) = P_{ei}(t) - P_{mi}$ the power deviation; $P_{ei}(t)$ the active electrical power; P_{mi} the mechanical input power; $e'_{qi}(t)$ the transient emf in the quadrature axis; $i_{di}(t)$ the direct axis current; $i_{qi}(t)$ the quadrature axis current; $v_i(t)$ the terminal voltage of the synchronous generator; $v_{di}(t)$ the direct axis terminal voltage; $v_{qi}(t)$ the quadrature axis terminal voltage; $v_{fi}(t)$ the control input of the excitation system; D_i the damping torque constant; H_i the inertia constant; T'_{d0i} the direct axis transient open circuit time constant; x_{di} the direct axis reactance; x'_{di} the direct axis transient reactance; x_{qi} the quadrature axis reactance; k_{ci} the gain of the excitation amplifier and B_{ij} the susceptance between i and j nodes. In addition, $v_{fi}(t)$ is constrained by

$$V_{mi} \le v_{fi}(t) \le V_{Mi}. \quad (12)$$

III. Voltage Controller Design

The design of the i-th voltage control scheme will be developed under the assumption of normal operating conditions of the power system. The first step is to write the differential input-output model with input $v_{fi}(t)$ and output $v_i(t)$. To this aim let us start by substituting (4)-(5) into (6)-(7) and bearing in mind that $\alpha_{ii}(t) = -B_{ii}$ it has

$$v_{di}(t) = x_{qi} \sum_{j=i}^{n} e'_{qj}(t)\, \beta_{ij}(t) \quad (13)$$

$$v_{qi}(t) = \big(1 + x'_{di}\, B_{ii}\big)\, e'_{qi}(t) - x'_{di}\, f_i(t) \quad (14)$$

with

$$f_i(t) = \sum_{j\neq i}^{n} e'_{qj}(t)\, \alpha_{ij}(t). \quad (15)$$

Solving (14) with respect to $e'_{qi}(t)$ yields

$$e'_{qi}(t) = \frac{1}{1 + x'_{di}\, B_{ii}}\Big(v_{qi}(t) + x'_{di}\, f_i(t)\Big). \quad (16)$$

Differentiating (14) with respect to time and using (3) one has

$$\frac{\mathrm{d}v_{qi}}{\mathrm{d}t}(t) = -\frac{1 + x'_{di}\, B_{ii}}{T'_{d0i}}\Big(e'_{qi}(t) + (x_{di} - x'_{di})\, i_{di}(t) - k_{ci}\, v_{fi}(t)\Big) - x'_{di}\, \frac{\mathrm{d}f_i}{\mathrm{d}t}(t). \quad (17)$$

The substitution of (4) and (16) into (17) after some manipulations yields

$$\frac{\mathrm{d}v_{qi}}{\mathrm{d}t}(t) = -\frac{1}{T'_{d0i}}\Big(1 - B_{ii}(x_{di} - x'_{di})\Big)\, v_{qi}(t) - \frac{x_{di}}{T'_{d0i}}\, f_i(t) + \frac{1 + x'_{di}\, B_{ii}}{T'_{d0i}} k_{ci}\, v_{fi}(t) - x'_{di}\, \frac{\mathrm{d}f_i}{\mathrm{d}t}(t). \quad (18)$$

Differentiating (6) one has

$$\frac{\mathrm{d}v_{di}}{\mathrm{d}t}(t) = x_{qi}\, \frac{\mathrm{d}i_{qi}}{\mathrm{d}t}(t) \quad (19)$$

while differentiating (8)

$$v_i(t)\, \frac{\mathrm{d}v_i}{\mathrm{d}t}(t) = v_{qi}(t)\, \frac{\mathrm{d}v_{qi}}{\mathrm{d}t}(t) + v_{di}(t)\, \frac{\mathrm{d}v_{di}}{\mathrm{d}t}(t) \quad (20)$$

and substituting the following expressions

$$v_{qi}(t) = v_i(t)\cos\phi_i(t) \quad (21)$$

$$v_{di}(t) = v_i(t)\sin\phi_i(t) \quad (22)$$

into (20) it results

$$\frac{\mathrm{d}v_i}{\mathrm{d}t}(t) = \cos\phi_i(t)\frac{\mathrm{d}v_{qi}}{\mathrm{d}t}(t) + \sin\phi_i(t)\frac{\mathrm{d}v_{di}}{\mathrm{d}t}(t) \quad (23)$$

where $\phi_i(t)$ is the phase displacement between the q_i-axis and $v_i(t)$ with $0 < \phi_i(t) < \pi/2$.

Now, substituting (18) and (19) into (23) using (21) one finally obtains

$$\frac{\mathrm{d}v_i}{\mathrm{d}t}(t) + a_{vi}(t)\, v_i(t) = k_{ci}\, b_{bi}(t)\, v_{fi}(t) + w_{vi}(t) \quad (24)$$

with

$$a_{vi}(t) = \frac{1 - B_{ii}(x_{di} - x'_{di})}{T'_{d0i}}\, \cos^2\phi_i(t) \quad (25)$$

$$b_{vi}(t) = \frac{1 + x'_{di}\, B_{ii}}{T'_{d0i}}\cos\phi_i(t) \quad (26)$$

$$w_{vi}(t) = \Big(-\frac{x_{di}}{T'_{d0i}} f_i(t) + x'_{di}\frac{\mathrm{d}f_i}{\mathrm{d}t}(t)\Big)\cos\phi_i(t) + x_{qi}\frac{\mathrm{d}i_{qi}}{\mathrm{d}t}(t)\sin\phi_i(t) \quad (27)$$

where $a_{vi}(t)$ and $b_{vi}(t)$ can be regarded as uncertain time-varying parameters. The susceptance B_{ii} is equal to zero in open-circuit condition while it is equal to $-1/(x'_{di} + x_{ti})$ in short-circuit condition, where x_{ti} denotes the reactance of the transformer. Based on this consideration, the uncertain parameters are constrained by

$$0 < a_{vi}(t) \le \frac{1}{T'_{d0i}}\Big(1 + \frac{x_{di} - x'_{di}}{x'_{di} + x_{ti}}\Big)$$

$$0 < b_{vi}(t) \le \frac{1}{T'_{d0i}}.$$

Looking at the expression (15) of the term $f_i(t)$ that appears in $w_{vi}(t)$, see (27), it can be recognized that $w_{vi}(t)$ takes into account the interactions between the i-th subsystem and the others $n-1$. In practice, the regulation and stabilization of the j-th subsystem ($j \neq i$) is viewed

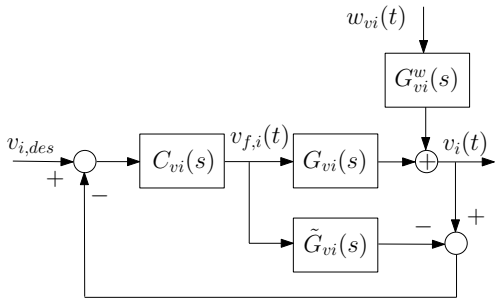

Fig. 1. Internal model control-based voltage control scheme.

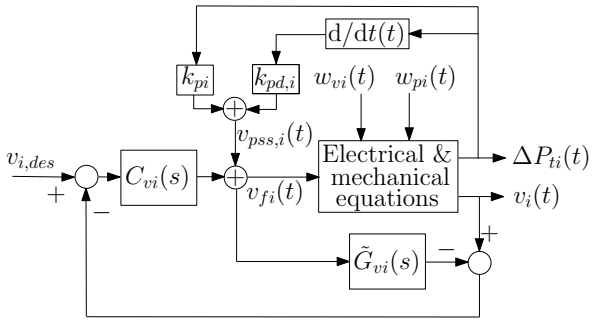

Fig. 2. Overall control scheme.

as a disturbance which affects the regulation of the i-th subsystem. Furthermore, since at the equilibrium point signals $e'_{qj}(t)$ and $i_{qi}(t)$ are constant, the amplitude of $w_{vi}(t)$ will be constant.

Denoting by $G_{vi}(s)$ the transfer function from $v_{fi}(t)$ to $v_i(t)$ obtained from model (24) and denoting by $\widetilde{G}_{vi}(s)$ an estimate of $G_{vi}(s)$, the internal model control-based design of the voltage controller is

$$C_{vi}(s) = F_i(s)\,\widetilde{G}_{vi}(s)^{-1} \tag{28}$$

where $F_i(s)$ makes $C_{vi}(s)$ realizable and $F_i(0) = 1$. The design of $F_i(s)$ may also be developed with the aim to impose a desired shape to the closed-loop response $v_i(t)$. The internal model control scheme is depicted in Figure 1 where $G^w_{vi}(s)$ is the transfer function from $w_{vi}(t)$ to $v_i(t)$

From the analysis of the scheme in Figure 1 it can be recognized that set-point tracking and asymptotic disturbance rejection are achieved regardless model mismatching between $G_{vi}(s)$ and $\widetilde{G}_{vi}(s)$.

IV. PSS Design

Considering a first-order approximation, the electrical power of the PSS can be expressed by

$$P_{pss,i}(t) \approx \frac{\partial P_{ei}}{\partial v_i}(t)\, v_{pss,i}(t) \tag{29}$$

in which $P_{pss,i}(t)$ represents the contribution, during transient, of the PSS to the rotor angle dynamics given by (2) and $v_{pss,i}(t)$ is the stabilizing signal output by the PSS. Accordingly, by adding in (2) the expression of $P_{pss,i}(t)$ given by (29) one has

$$\frac{\mathrm{d}\Delta\omega_i}{\mathrm{d}t}(t) = -\frac{D_i}{H_i}\,\Delta\omega_i(t) - \frac{\omega_0}{H_i}\Big(\Delta P_{ei}(t) + \frac{\partial P_{ei}}{\partial v_i}(t)\, v_{pss,i}(t)\Big). \tag{30}$$

Let us define

$$\Delta P_{ti}(t) = \Delta P_{ei}(t) + \frac{\partial P_{ei}}{\partial v_i}(t)\, v_{pss,i}(t) \tag{31}$$

the actual measurable power deviation which coincides with $\Delta P_{ei}(t)$ when $v_{pss,i}(t) = 0$.

Substituting (21) and (22) in (11), the active electrical power becomes

$$P_{ei}(t) = \frac{v_i(t)\, e'_{qi}(t)}{x'_{di}}\,\sin\phi_i(t) - \frac{(x_{qi} - x'_{di})}{2\,x_{qi}\,x'_{di}} v_i^2(t)\,\sin(2\,\phi_i(t)). \tag{32}$$

Since P_{mi} is constant, differentiating (32) it has

$$\frac{\mathrm{d}\Delta P_{ei}}{\mathrm{d}t}(t) = \frac{\partial P_{ei}}{\partial \phi_i}(t)\Delta\omega_i(t) + w_{pi}(t) \tag{33}$$

with

$$w_{pi}(t) = \frac{\partial P_{ei}}{\partial v_i}(t)\,\frac{\mathrm{d}v_i}{\mathrm{d}t}(t) + \frac{\partial P_{ei}}{\partial e'_{qi}}(t)\,\frac{\mathrm{d}e'_{qi}}{\mathrm{d}t}(t) - \frac{\partial P_{ei}}{\partial \phi_i}(t)\,\frac{\mathrm{d}\gamma_i}{\mathrm{d}t}(t) \tag{34}$$

with $\gamma_i(t) = \delta_i(t) - \phi_i(t)$.

From (33) it has

$$\Delta\omega_i(t) = \Big(\frac{\partial P_{ei}}{\partial \phi_i}(t)\Big)^{-1}\Big(\frac{\mathrm{d}\Delta P_{ei}}{\mathrm{d}t}(t) - w_{pi}(t)\Big). \tag{35}$$

Now, let us define the following control law

$$v_{pss,i}(t) = k_{pi}\,\Delta P_{ti} + k_{pd,i}\,\frac{\mathrm{d}\Delta P_{ti}}{\mathrm{d}t}(t). \tag{36}$$

Substituting for ΔP_{ti} and its first order derivative obtained by (31), neglecting the higher order term

$$\frac{\mathrm{d}}{\mathrm{d}t}(t)\Big(\frac{\partial P_{ei}}{\partial v_i}(t)\, v_{pss,i}(t)\Big)$$

it is possible to rewrite control law (36) as

$$v_{pss,i}(t) = \frac{k_{pi}\,\Delta P_{ei}}{1 - k_{pi}\dfrac{\partial P_{ei}}{\partial v_i}(t)} + \frac{k_{pd,i}}{1 - k_{pi}\dfrac{\partial P_{ei}}{\partial v_i}(t)}\,\frac{\mathrm{d}\Delta P_{ei}}{\mathrm{d}t}(t). \tag{37}$$

The substitution of (35) and (37) in (30) finally gives the closed-loop differential model in the machine variable $\Delta P_{ei}(t)$ and disturbance $w_{pi}(t)$.

$$\frac{\mathrm{d}^2\Delta P_{ei}}{\mathrm{d}t^2}(t) + \Big(\frac{D_i}{H_i} + \frac{\omega_0}{H_i}\frac{\dfrac{\partial P_{ei}}{\partial v_i}(t)\dfrac{\partial P_{ei}}{\partial \phi_i}(t)}{1 - k_{pi}\dfrac{\partial P_{ei}}{\partial v_i}(t)}k_{pd,i}\Big)\frac{\mathrm{d}\Delta P_{ei}}{\mathrm{d}t}(t)$$

$$+\frac{\omega_0}{H_i}\,\frac{\partial P_{ei}}{\partial \phi_i(t)}\,\frac{1}{1 - k_{pi}\dfrac{\partial P_{ei}}{\partial v_i}(t)}\Delta P_{ei}(t) - \frac{\mathrm{d}w_{pi}}{\mathrm{d}t}(t)$$

$$-\frac{D_i}{H_i}\,w_{pi}(t) = 0. \tag{38}$$

From the expression of the input disturbance $w_{pi}(t)$ given by (34) it can be recognized that $w_{pi}(t)$ takes into account the mutual influence between the electrical and mechanical dynamics of the same subsystem. In particular, it can be viewed as an "electrical disturbance" which affects the swings damping. Then, to mitigate the effects of $w_{pi}(t)$ on $\Delta\omega_i(t)$, it is advisable to choose values of k_{pi} and $k_{pd,i}$ so as to realize a filtering action of $w_{pi}(t)$ across the typical frequencies of about few radiants per second. Then, higher values of k_{pi} and $k_{pd,i}$, compatibly with the achievable performance and imposed limits (12), would improve swings damping but may lead to undesired values of overshoots of $v_i(t)$. In fact, higher values of k_{pi} and $k_{pd,i}$ result into an increased amplitude of $v_{pps,i}(t)$, see (36), and, consequently of $v_{fi}(t)$, see Figure 2.

At the equilibrium point it has $\lim_{t\to\infty} w_{pi}(t) = 0$. Since control law (36) guarantees asymptotic stability of the closed-loop system (38), it results $\lim_{t\to\infty} \Delta P_{ei}(t) = 0$, and, consequently, from (37) $\lim_{t\to\infty} v_{pss,i}(t) = 0$. Hence $\lim_{t\to\infty} \Delta P_{ti}(t) = 0$

Signal $v_{pss,i}(t)$ requires the availability of $\mathrm{d}\Delta P_{ti}(t)/\mathrm{d}t$. It can be obtained, for example, by using a tracking differentiator which can track the differential of the input signal with high precision and fast converging speed [15].

Finally it is important to remark that the proposed design is effective if each i-th controller stabilizes the i-th synchronous generator. This assumption is quite reasonable and it is fulfilled when the oscillation phenomena are local, that is when oscillation amplitude is very large for few generators, that are close to each other and form a single area, and small for the generators of other areas. On the other hand, when facing inter-area oscillation phenomena, different approaches should be adopted, see for example [12].

V. Case study

The simulated power system is shown in Fig. 3. It is a three-phase 220 kV-50 Hz network which is connected at node 1 to a larger system which is represented by a network equivalent with a short-circuit power equal to 1000 MVA and an open-circuit voltage equal to 1.01 p.u. (per-unit) on a 220 kV base. The assumed short-circuit power value is much lower than the typical values in HV nodes, so as to considering critical conditions for stability studies. The 220 kV overhead transmission lines present the following values per length unit: series resistance equal to 84 mΩ/km, series inductance equal to 1.3 mH/km and shunt capacitance equal to 8.6 nF/km. At nodes 3 and 5, two loads, named respectively Q_1 and Q_2, are connected both with a power factor equal to 0.9 and rated power equal to 350 MW. At nodes 2, 4 and 6 of the network are connected three synchronous generators whose parameters are listed in Table I. The simulation is developed using the PSCAD/EMTDC software, a simulation tool for analyzing power systems transients(https://pscad.com/).

In the voltage controller design, assuming

$$\widetilde{G}_{vi}(s) = \frac{k_{ci}\,\tilde{b}_{vi}}{s + \tilde{a}_{vi}}$$

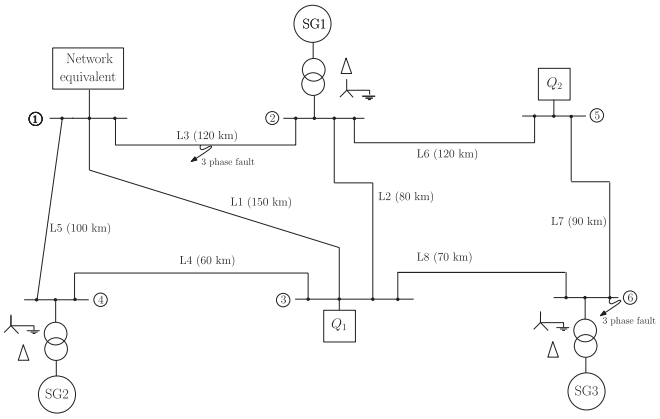

Fig. 3. Simulated power system.

TABLE I
Data of the synchronous generators.

Parameter	SG1	SG2	SG3
Type of rotor	Massive	Salient pole	Massive
S_n [MVA]	370	125	190
v_n [kV]	25	16	20
f_n [Hz]	50	50	50
H [s]	7.5	7	7
D [p.u.]	4	2	2
x_d [p.u.]	1.9	1	2
x'_d [p.u.]	0.302	0.3	0.2
x''_d [p.u.]	0.204	0.2	0.15
x_q [p.u.]	1.7	0.7	2
x'_q [p.u.]	0.5	–	–
x''_q [p.u.]	0.3	0.2	0.15
T'_{d0} [s]	8	5	7
T''_{d0} [s]	0.027	0.06	0.03
T'_q [s]	0.235	–	–
T''_q [s]	0.012	0.06	0.06
x_t [p.u.]	0.1	0.1	0.1

the following parameter values have been chosen

$$\tilde{a}_{v1} = 0.1905 \quad \tilde{a}_{v2} = 0.2821 \quad \tilde{a}_{v3} = 0.3528$$
$$\tilde{b}_{v1} = 0.0668 \quad \tilde{b}_{v2} = 0.1072 \quad \tilde{b}_{v3} = 0.0875$$

which have been obtained from (25)–(26) assuming $B_{ii} = -1.0$ p.u. and $\phi_i = 40$ degrees. Moreover it is set $k_{ci} = 1.0$.

Concerning filter $F_i(s)$ in (28) it is chosen the following structure

$$F_i(s) = 40\,\frac{\tilde{a}_{vi}^2}{(s + 2\,\tilde{a}_{vi})\,(s + 20\,\tilde{a}_{vi})}.$$

In the PSS design the following values for the parameters in the closed-loop system (38) have been assumed

$$\frac{\partial P_{e1}}{\partial v_1} = 0.18 \quad \frac{\partial P_{e2}}{\partial v_2} = 0.9 \quad \frac{\partial P_{e3}}{\partial v_3} = 0.15$$
$$\frac{\partial P_{e1}}{\partial \phi_1} = 2.1 \quad \frac{\partial P_{e2}}{\partial \phi_2} = 2.3 \quad \frac{\partial P_{e3}}{\partial \phi_3} = 2.8\,.$$

Two different PSS, named PSS_A and PSS_B have been designed. For each of two PSS and for each synchronous generator, the corresponding gains are reported in Table II.

TABLE II

PARAMETERS OF THE TWO PSS DESIGNS.

PSS	Generator	k_{pi}	$k_{pd,i}$
PSS_A	SG1	-41	5.1
	SG2	-9.4	0.6
	SG3	-21	2.6
PSS_B	SG1	-120	10
	SG2	-80	8
	SG3	-80	8

In particular, the gains of PSS_B are higher than the ones of PSS_A, so as to improve rejection of $w_{pi}(t)$.

In the first simulation the symmetrical three-phase short circuit fault occurs at the middle of the transmission line L_3. The fault appears at time $t = 1$ s and at time $t = 1.2$ s is cleared. The fault clearance causes the exclusion of the line L_3 so that the post-fault operating condition is different from the pre-fault one. The results of the simulation are reported in Figs. 4–5, respectively for PSS_A and PSS_B.

From the simulation results it is possible to state that swings damping and voltage regulation are satisfactory achieved after fault clearance by both designs. Comparing the two Figures, it is apparent that, as expected, PSS_B presents a better damping of mechanical oscillations. However, such an improvement has a drawback in terms of performance of the voltage regulation. Indeed the overshoot of voltages above the reference value (assumed equal to 1.02 p.u. for all the generators) in the case of PSS_B is unacceptable in actual power systems. For this latter reason PSS_A design must be preferred.

In the second simulation the symmetrical three-phase short circuit fault occurs at busbar 6 where SG3 is connected. The fault always appears at time $t = 1$ s and at time $t = 1.2$ s is cleared. The results of the simulation are reported in Fig. 6 in the case of PSS_A design. Due to the fault position, SG3 is subject to a larger swing and to a deeper voltage sag with respect to SG1 and SG2. Comparing the results with the ones of the first simulation reported in Fig. 4, it is important to note that, after the fault is cleared, the time evolutions are quite similar and the system restores the pre-fault conditions in about the same time interval.

VI. CONCLUSIONS

The decentralized control-based design of a voltage controller and a PSS has been presented to achieve transient stability and voltage regulation in multimachine power systems. The approach is simple to apply and is sequentially developed in the sense that each controller is designed regardless from the presence of the other one. The voltage controller is designed according to the internal model control while the PSS with the aim to reduce the influence of the voltage regulation on the swing damping. Despite the design has been developed under the assumption of noninteractive controllers, the simulation results have indicated that the controllers can provide satisfactory transient control when the system suffers from the uncertainties and disturbances.

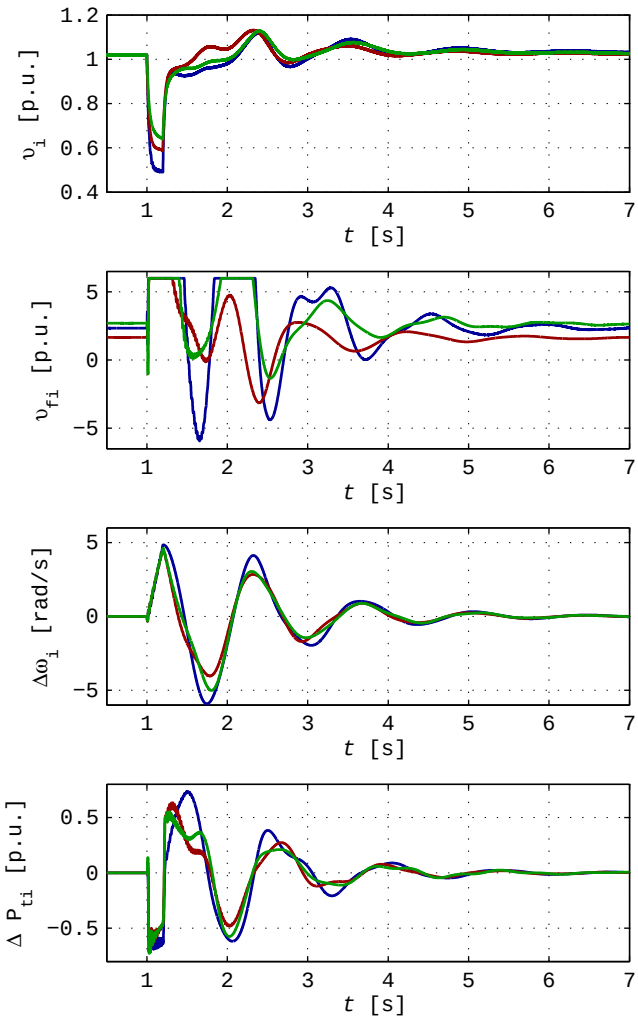

Fig. 4. Three-phase short-circuit on line L_3: case of PSS_A (plots: SG1 blue, SG2 red, SG3 green).

REFERENCES

[1] P.M. Anderson and A.A. Fouad, *Power System Control and Stability*, IEEE Press, Inc, New York, USA, 1994.

[2] V. Bandal, and B. Bandyopadhyay, "Robust decentralised output feedback sliding mode control technique-based power system stabiliser (PSS) for multimachine power system," *Control Theory and Applications*, **1**(5), pp. 1512-1522, 2007.

[3] G. K. Befekadu, and I. Erlich, "Robust Decentralized Controller Design for Power Systems Using Matrix Inequalities Approaches," *IEEE Power Engineering Society General Meeting*, 2006.

[4] Y. Guo, D.J. Hill and Y. Wang, "Nonlinear decentralized control of large-scale power systems," *Automatica*, **36**(9), pp. 1275–1289, 2000.

[5] Y. Guo, Y. Wang and D.J. Hill, "Nonlinear Output Stabilization Control for Multimachine Power Systems," *IEEE Trans. on Circuits and Systems, Part 1*, **47**(1), pp. 46–53, 2000.

[6] H. Huerta, A.G. Loukianov, and Jose M. Cañedo, "Decentralized sliding mode block control of multimachine power systems," *International Journal of Electrical Power and Energy Systems*, **32**(1), pp. 1-11, 2010.

[7] L. Jiang, Q.H. Wu, and J.Y. Wen, "Decentralized Nonlinear Adaptive Control for Multimachine Power Systems Via High-Gain Perturbation Observer," *IEEE Transactions on Circuits and Systems*, **51**(10), pp. 2052–2059, 2004.

[8] K. Kalsi, J. Lian and S.H. Żak, "Decentralized Control of Multimachine Power Systems," *18th IEEE American Control Conference*, pp. 2122–2127, 2009.

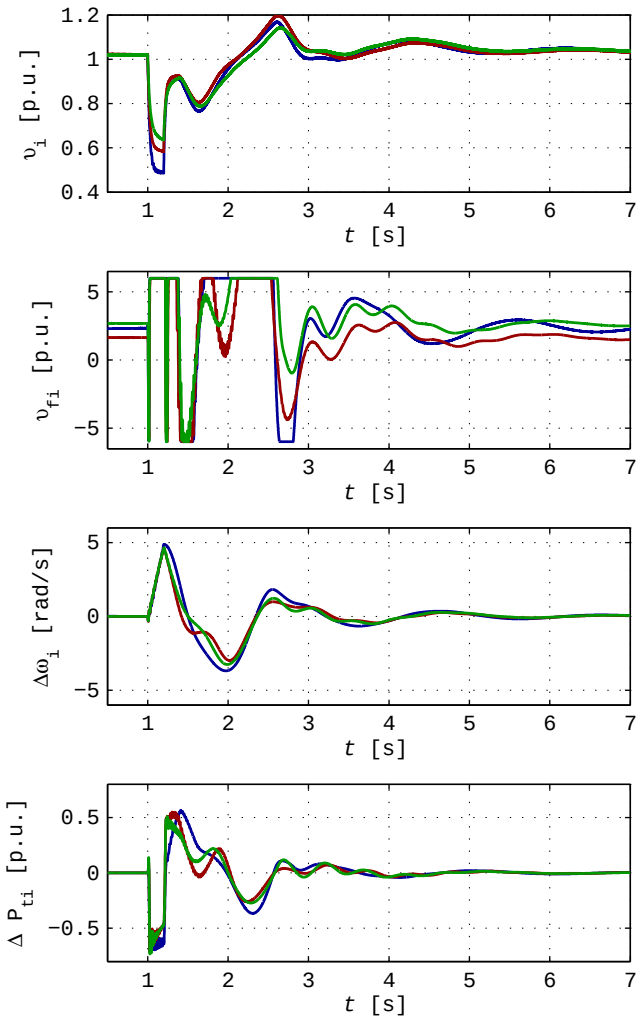

Fig. 5. Three-phase short-circuit on line L_3: case of PSS_B (plots: SG1 blue, SG2 red, SG3 green).

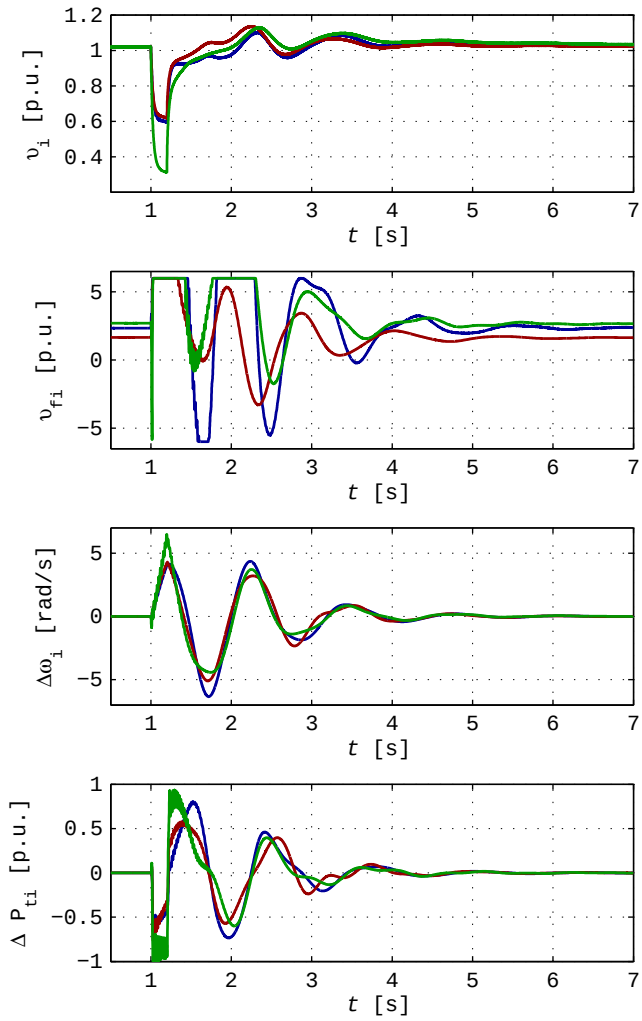

Fig. 6. Three-phase short-circuit at busbar 6: case of PSS_A (plots: SG1 blue, SG2 red, SG3 green).

[9] P. Kundur, *Power System Stability and Control*, McGraw-Hill, New York, USA, 1994.

[10] R. Marconato, *Electric Power System: Background and Basic Concepts*, CEI Italian Electrotechnical Committee, Second Edition, Vol.1, Milano, I, 2002.

[11] M. Ouassaid, M. Cherkaoui, and M. Maaroufi, "Nonlinear Decentralized Control of a Multimachine Power system," *18th IEEE Mediterranean Conference on Control & Automation*, pp. 111–116, 2010.

[12] F. Okou and L.-A. Dessaint and O. Akhrif "Power Systems Stability Enhancement Using a Wide-Area Signals Based Hierarchical Controller," *IEEE Trans. on Power Systems*, **20**(3)1465–1477, 2005.

[13] J. Fernàndez-Vargas, and Tadeusz Niewierowicz, "Excitation control for multimachine power systems," *Electric Power and Energy Systems*, **76**(6-7), pp. 476-484, 2006.

[14] Z. Xi, D. Cheng, Q. Lu, and S. Mei, "Nonlinear decentralized controller design for multimachine power systems using Hamiltonian function method," *Automatica*, **38**(3), pp. 527-534, 2002.

[15] X. Wang, S. Yau and J. Huang, "A study of tracking differentiator," *39th IEEE International Conference on Decision and Control*, pp. 4783–4784, 2000.

[16] C. Zhu, R. Zhou, and Y. Wang, "A new decentralized nonlinear voltage controller for multimachine power systems," *International Conference on Control and Automation*, pp. 525–530, 2003.